

Supplementary Information

Synergistic effect of graphene and ionic liquid containing phosphonium on the thermal stability and flame retardancy 5 of polylactide

Haoguan Gui ^a, Pei Xu ^{a,b*}, Yadong Hu ^a, Jie Wang ^a, Xuefeng Yang ^a, Ali Bahader ^a,
Yunsheng Ding ^{a,b*}

^a Department of Polymer Science and Engineering, Hefei University of Technology, Hefei, 230009, P.
10 R. China.

^b Anhui Key Laboratory of Advanced Functional Materials and Devices, Hefei University of
Technology, Hefei, 230009, China.

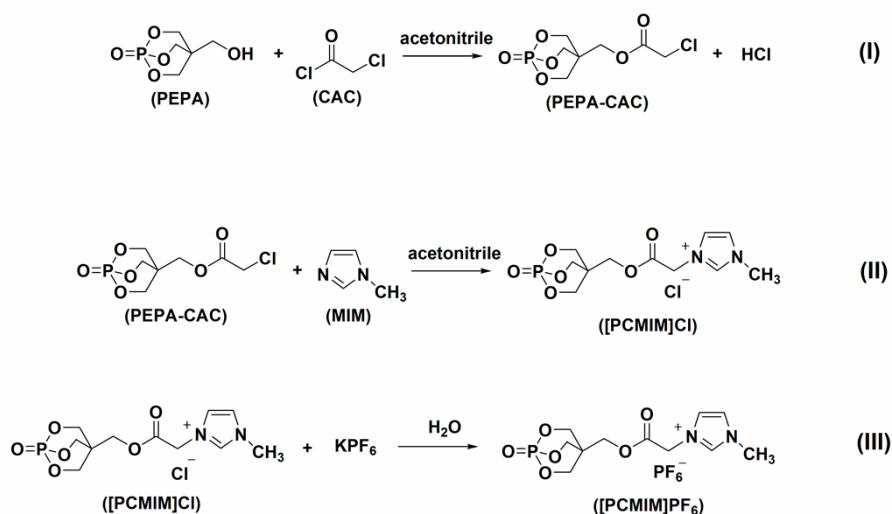
Corresponding author Tel: +86 551 62901545;

E-mail: Pei Xu (chxuper@hfut.edu.cn);

15 Yunsheng Ding (dingys@hfut.edu.cn)

1. The synthesis of [PCMIM]PF₆

The synthesis was simplified and optimized when compared with our previous work.¹ Commercial 1-oxo-4-methoxy-2,6,7-trioxa-1-phosphabicyclo[2,2,2]octane (PEPA) (98%) was supplied by Shanghai Longsheng Chemical Co.,Ltd., China. Chloroacetyl chloride (CAC), 1-Methylimidazole (MIM), Potassium hexafluorophosphate (KPF₆), cyclohexane and acetonitrile were purchased from Sinopharm Chemical Reagent Co., Ltd., China. All chemical reagents were of reagent grade and were used with further purification.



Scheme S1. The synthesis route of [PCMIM]PF₆.

10

1.1 The purification of PEPA

In a 250 ml beaker, 36.01 g (0.20 mol) of the received PEPA (white solid) was washed with hexane for 3 times. The powdery product was dried at 70 °C under vacuum for 12 h. Mp (Melting Point) 210±1 °C. The FTIR (Fourier Transform Infrared Spectroscopy) and ¹H NMR (Nuclear Magnetic Resonance) spectra of PEPA are shown in Fig. S1 and Fig. S2 respectively.

20

¹H NMR (Varian VNMRS 600 MHz NMR spectrometer, USA) (400 MHz, *d*⁶-DMSO) δ (ppm): 5.10 (t,

1H, OH); 4.58 (d, 6H, P–O–CH₂); 3.30 (t, 2H, CH₂–OH).

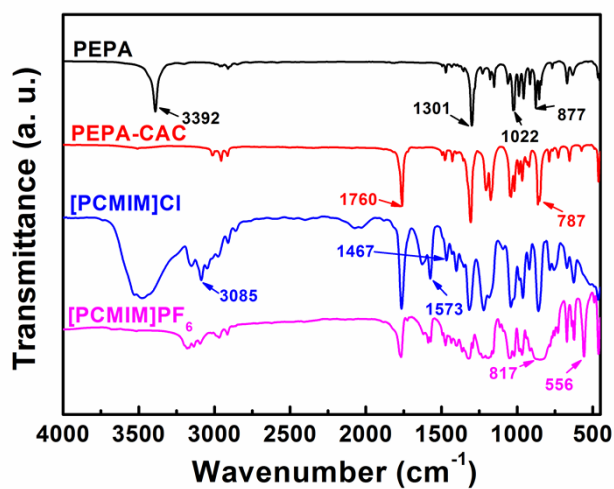
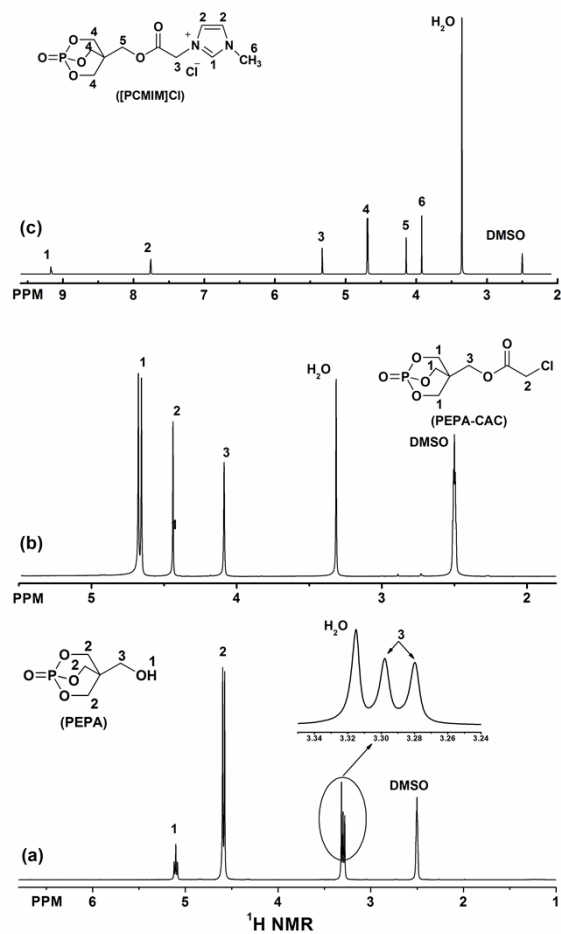


Fig. S1. The FTIR spectra of PEPA, PEPA-CAC, [PCMIM]Cl and [PCMIM]PF₆.



5

Fig. S2. The ¹H NMR spectra for (a) PEPA, (b) PEPA-CAC and (c) [PCMIM]Cl.

1.2 The synthesis of PEPA-CAC

In a 250 ml three-necked round-bottom flask, equipped with the magnetic stirring apparatus, reflux condenser, addition funnel and nitrogen protective device, 27.01 g (0.15 mol) PEPA and 100 ml acetonitrile were added. Within an hour, 33.89 g (0.30 mol) CAC, at 35 °C, was slowly dripped to the system; keeping the reaction going at 60 °C for 12 h under the purging of nitrogen. The reaction mixture was concentrated by rotary evaporator, and the crude product was precipitated in deionized water, purified, then dried to get PEPA-CAC (84% yield) in vacuum drier at 70 °C for overnight. The synthesis route is illustrated in Scheme S1(I), the FTIR and ¹H NMR spectra of PEPA-CAC are shown in Fig. S1 and Fig. S2 respectively.

10

FTIR (KBr, cm⁻¹): 1760 (C=O, stretching); 787 (C-Cl, stretching).

¹H NMR (400 MHz, *d*⁶-DMSO) δ (ppm): 4.66 (d, 6H, P-O-CH₂); 4.44 (s, 2H, CH₂-Cl); 4.09 (s, 2H, C-CH₂-OCO).

15

1.3 The synthesis of [PCMIM]Cl

In a 250 ml three-necked round-bottom flask, equipped with the magnetic stirring apparatus, reflux condenser and nitrogen protective device, 30.79 g (0.12 mol) PEPA-CAC and 12.31 g (0.15 mol) MIM were dissolved in 120 ml acetonitrile. White with light universal-grey solid confirmed as [PCMIM]Cl was gathered from the acetonitrile phase after reacting at 70 °C for 12 h. This solid was washed with acetonitrile until pellucid filtering liquid, collected by filtration and dried under vacuum at 70 °C to a constant weight (95% yield). The synthesis route is illustrated in Scheme S1(II), the FTIR and ¹H NMR spectra of [PCMIM]Cl are shown in Fig. S1 and Fig. S2 respectively.

25 FTIR (KBr, cm⁻¹): 3085 (=C-H, stretching); 1573, 1467 (skeleton vibration of imidazole ring). The stretching vibration of -O-H was observed at 3486 cm⁻¹ because of the super-hydrophilic of [PCMIM]Cl which can be wetted easily in atmosphere.

¹H NMR (400 MHz, *d*⁶-DMSO) δ (ppm): 9.18 (s, 1H, NCHN); 7.76 (d, 2H, NCHCH); 5.33 (s, 2H, N-CH₂); 3.93 (s, 3H, N-CH₃).

30

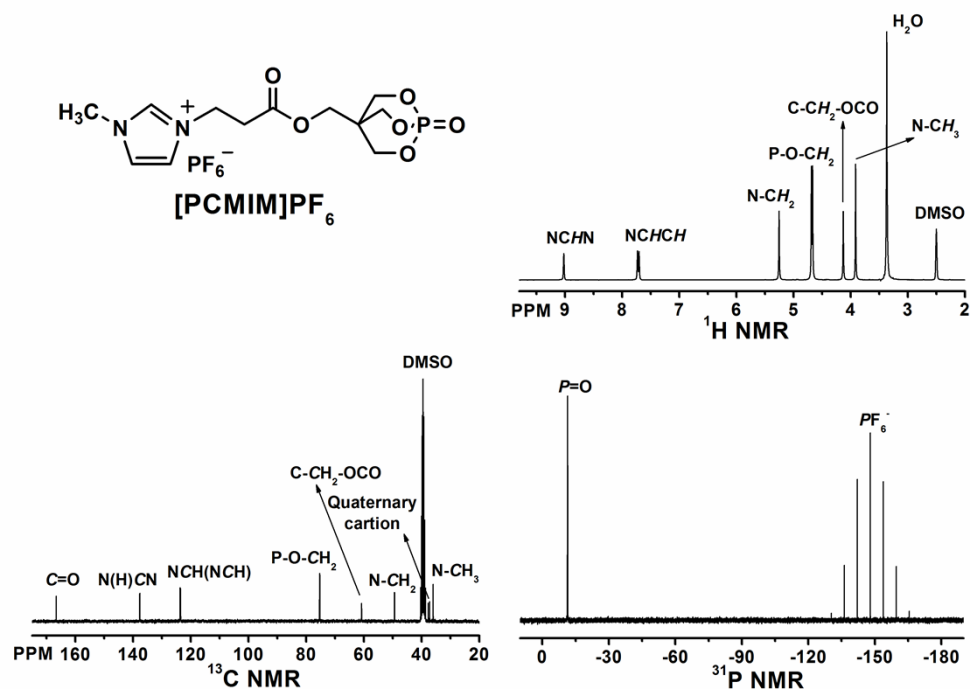


Fig. S3. ^1H , ^{13}C and ^{31}P NMR spectra of $[\text{PCMIM}]\text{PF}_6$.

1.4 The synthesis of $[\text{PCMIM}]\text{PF}_6$ ²

5 In a 500 ml three-necked round-bottom flask, equipped with the magnetic stirring apparatus and reflux condenser, 33.87 g (0.10 mol) $[\text{PCMIM}]\text{Cl}$ was dissolved in 200 ml deionized water, and 120 ml (1 mol/l) KPF_6 aqueous solution, at room temperature, was slowly dripped to the flask. $[\text{PCMIM}]\text{PF}_6$, Mp 145 ± 1 °C, was precipitated as white and loosened solid after stirring for 8 h. This solid was washed with deionized water, collected by filtration and dried under vacuum at 70 °C for 24 h (87% yield). The

10 successful synthesis of $[\text{PCMIM}]\text{PF}_6$ is confirmed from FTIR, ^1H NMR, ^{13}C NMR and ^{31}P NMR analyses. The synthesis route is illustrated in Scheme S1(III), Fig. S1 shows the FTIR spectrum of $[\text{PCMIM}]\text{PF}_6$ and Fig. S3 diagrams the ^1H , ^{13}C and ^{31}P NMR spectra.

FTIR (KBr, cm^{-1}): 817 (P–F, stretching); 556 (P–F, bending).

15

^1H NMR (400 MHz, d^6 -DMSO) δ (ppm): 9.02 (s, 1H, NCHN); 7.73 (d, 2H, NCHCH); 5.25 (s, 2H, N- CH_2); 4.66 (d, 6H, P-O- CH_2); 4.13 (s, 2H, C- CH_2 -OCO); 3.91 (s, 3H, N- CH_3). ^{13}C NMR (400 MHz, d^6 -DMSO) δ (ppm): 166.60 (C=O); 137.64 (N(H)CN); 123.64 (NCH); 123.47 (NCH); 75.28 (P-O- CH_2); 60.79 (C- CH_2 -OCO); 49.32 (N- CH_2); 37.39 (quaternary carbon); 35.94 (N- CH_3). ^{31}P NMR

(400 MHz, d^6 -DMSO) δ (ppm): -11.70 (P=O); and septet signal at around -147.98 ppm for PF_6^- .

2. Preparation of the ionic liquid-functionalized graphene (GIL)

Fig. S4 presents the FTIR spectra of the Gra, GIL and $[\text{PCMIM}]\text{PF}_6$. In the GIL composites, characteristic peaks (1573 and 1467 cm^{-1}) for the imidazolium cation of IL and stretching vibration (817 cm^{-1}) and bending vibration (556 cm^{-1}) for the hexafluorophosphate anion of IL are observed, which indicates that IL molecules have been successfully attached onto the Gra sheets.

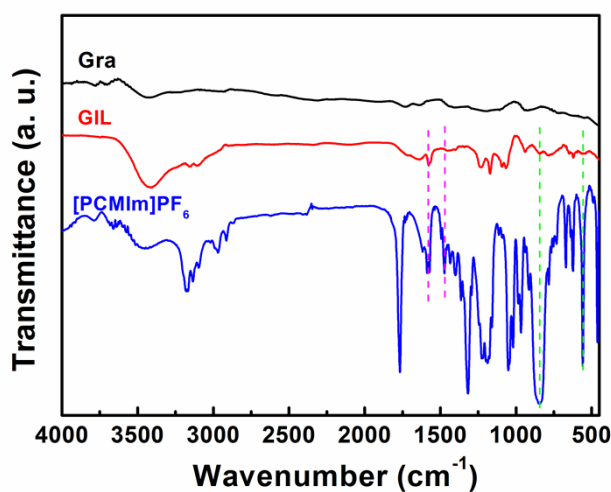


Fig. S4. The FTIR spectra of the Gra, GIL and $[\text{PCMIM}]\text{PF}_6$.

10

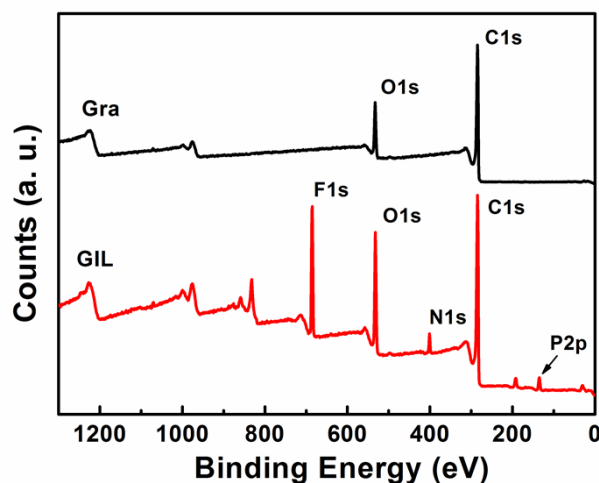


Fig. S5. XPS spectra of Gra and GIL.

To verify the interaction between the ionic liquid and graphene, X-ray Photoelectron Spectroscopy

(XPS) was applied in characterization of the two samples. It is found that two bands located at around 285.1 and 532.5 eV which attributed to C1s and O1s are observed, respectively (shown in Fig. S5). The peaks at 134.2, 401.0 and 685.4 eV are attributed to P2p, N1s and F1s, respectively, so that the IL was determined in the surface of GIL. This is further confirmed by the C1s core level spectra of GIL shown in Fig. S6 (b), where the content of N-C=N bond centered at 287.2 eV³. Three peaks appear in both Gra and GIL at 284.7, 286.2 and 287.7 eV, which are associated with C-C/C=C, C-O and C=O bands in graphene-based materials⁴. Moreover, the peak intensity of C-O and C=O in the C1s spectrum of GIL is a bit stronger than that of Gra, due to the existence of ester bond in the IL.

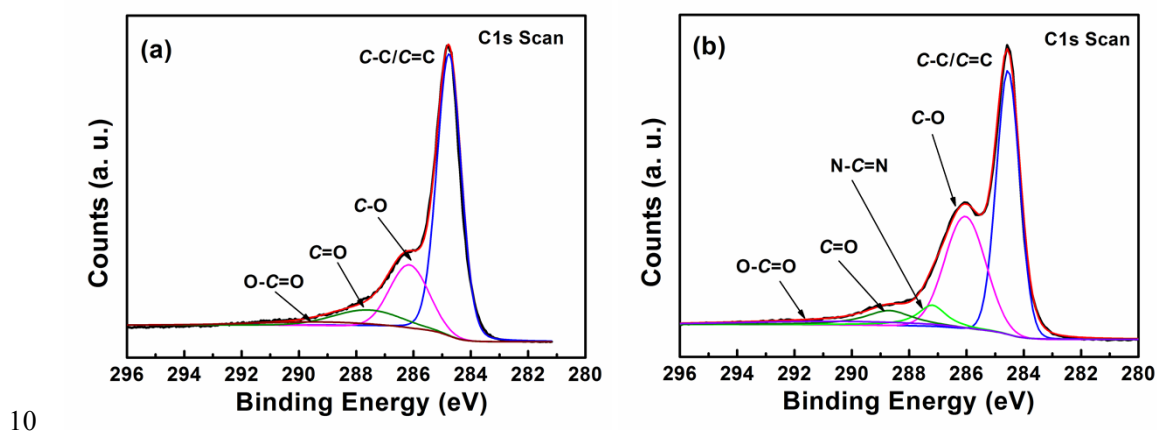


Fig. S6. C1s spectra of (a) Gra and (b) GIL.

3. The synergistic effects of graphene and ionic liquid on the thermal degradation of PLA

The calculated curve is a linear combination of the TGA curves of PLA, IL and Gra based on their weight percentages, which is representative of a non-interacting behavior among the individual components.⁵ As shown in Fig. S7, it can be seen that the experimental TGA curve of PLA/4GIL exhibits much higher thermal stability and larger amount of char residues in comparison with the calculated curves of PLA/1Gra, PLA/3IL and PLA/4GIL. For example, the $T_{initial}$ and T_{max} for PLA/4GIL could reach up to 331.4 °C, 364.5 °C from the experimental curve, while the calculated ones only show as 319.1 °C and 349.8 °C, respectively. Similarly, the char residue at 700 °C of experimental curve of PLA/4GIL also exhibits a much higher value of 9.0 wt %, while the calculation data for PLA/1Gra, PLA/3IL and PLA/4GIL are only 1.9 wt %, 2.1 wt % and 3.6 wt %, respectively. It

demonstrates that there is an obvious synergistic effect between IL and Gra, which could improve the thermal stability of PLA and promote PLA/GIL nanocomposites to form more chars. The chars can inhibit the releasing of combustible gas, and the heat flow during combustion causes high LOI value and V-0 rating. ⁶

5

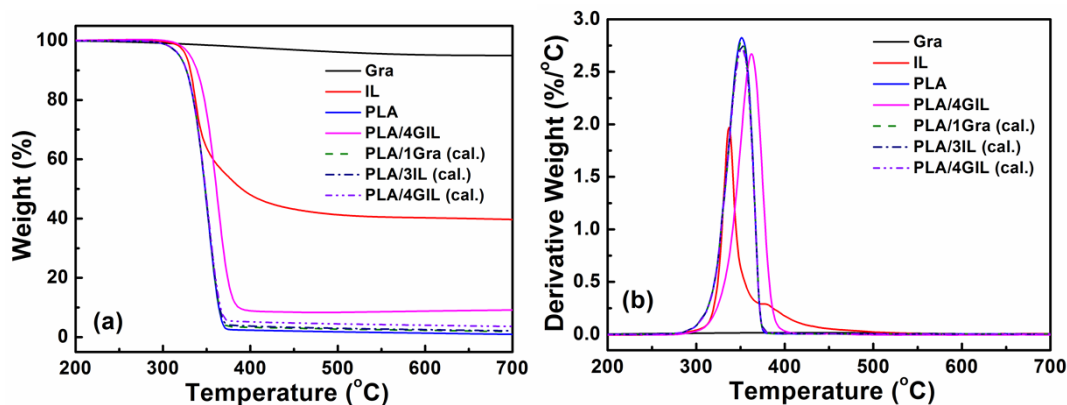


Fig. S7. (a) TGA and (b) DTG curves of Gra, IL, PLA, PLA/4GIL and PLA/1Gra (cal.), PLA/3IL (cal.), PLA/4GIL (cal.).

10

4. Thermal oxidative degradation of PLA/Gra and PLA/GIL nanocomposites

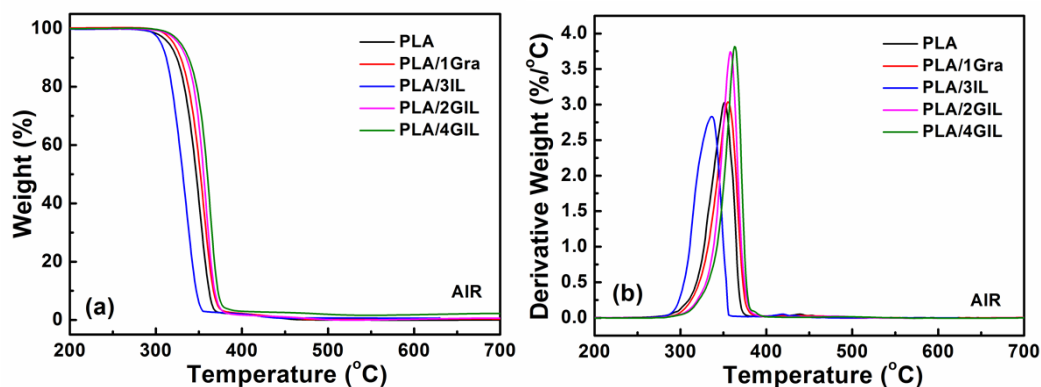


Fig. S8. (a) TGA and (b) DTG curves of PLA/Gra, PLA/IL and PLA/GIL nanocomposites in air.

15 Fig. S7 shows thermo-oxidative degradation curves of neat PLA and the nanocomposites experimented under the air atmosphere condition. It was found that the TGA and DTG curves under the air atmosphere were completely different from those under the nitrogen gas condition, which stems from that oxygen in air played an important role in the thermal oxidative degradation. The main thermo-

oxidative degradation of neat PLA occurred at about 346.3 °C and was climbed to about 354.6 °C with the addition of 1 wt % graphene (sample PLA/1Gra), while an around 12 °C and 17 °C improvement for PLA/2GIL and PLA/4GIL, respectively. And there is more than 15 °C decrease for PLA/3IL due to the catalytic thermal degradation effect of IL. Overall, the thermo-oxidative degradation temperatures of neat PLA and the nanocomposites under the air atmosphere are found to be lower than the corresponding degradation temperatures under the nitrogen condition. However, it should be mentioned that the decomposition rate of thermo-oxidative degradation is much quicker than that under the inert nitrogen condition, especially for the samples, PLA/2GIL and PLA/4GIL. Similar phenomenon is shown in the CCT test which result from catalytic action of IL in the thermo-oxidative degradation of PLA

References

1. X. Yang, N. Ge, L. Hu, H. Gui, Z. Wang and Y. Ding, *Polymers for Advanced Technologies*, 2013, **24**, 568-575.
2. J. P. Hallett and T. Welton, *Chemical Reviews*, 2011, **111**, 3508-3576.
3. C. Gabler, N. Dörr and G. Allmaier, *Tribology International*, 2014, **80**, 90-97.
4. Y. Fu, J. Zhang, H. Liu, W. C. Hiscox and Y. Gu, *Journal of Materials Chemistry A*, 2013, **1**, 2663-2674.
5. S. Ran, Z. Guo, C. Chen, L. Zhao and Z. Fang, *Journal of Materials Chemistry A*, 2014, **2**, 2999-3007.
6. C.-H. Ke, J. Li, K.-Y. Fang, Q.-L. Zhu, J. Zhu, Q. Yan and Y.-Z. Wang, *Polymer Degradation and Stability*, 2010, **95**, 763-770.